# 1.8 CLOUD PROPERTIES DERIVED FROM VIRS FOR CERES

Patrick Minnis*, David F. Young[1], Bruce A. Wielicki[1]
Atmospheric Sciences, NASA Langley Research Center, Hampton, VA

Patrick W. Heck
Analytical Services and Materials, Inc., Hampton, VA

Sunny Sun-Mack, Tim D. Murray
Science Applications International Corporation, Hampton, Virginia

## 1. INTRODUCTION

Cloud microphysical properties such as effective particle size, phase, and optical depth and macrophysical properties such as altitude and fractional coverage provide the critical links between the hydrological cycle and the effect of clouds on the radiation budget. The Clouds and Earth's Radiant Energy System (CERES; Wielicki et al., 1998) is the first project devoted to simultaneous determination of cloud properties and the broadband radiation budget. This paper briefly describes the methodology of the CERES daytime cloud property retrieval subsystem and presents the first results of its application to the fully calibrated, 2-km resolution Visible and Infrared Scanner (VIRS) on the 35°-inclined-orbit Tropical Rainfall Measuring Mission (TRMM) satellite. The distributions of cloud phase, effective particle sizes, liquid water path, ice water path, heights, and fractional coverage are derived from January 1998 data.

## 2. DATA

The 2-km resolution VIRS satellite measures radiances at 0.65, 1.6, 3.75, 10.8, and 12.0 μm. It scans in a cross-track direction out to a nadir angle of 45°, which translates to a maximum viewing zenith angle $\theta$ of 48°. The TRMM orbit gives the VIRS a viewing perspective distinctly different from either geostationary or Sun-synchronous satellites. It samples all local times of day over a 46-day period. At the Equator, this sampling is evenly distributed over the period, but at higher latitudes, the sampling is primarily in darkness for 3 weeks followed by 3 weeks of sunlight. For each VIRS pixel, the CERES processing system assigns a scene classification that is some category of clear or cloudy (Trepte et al., 1999), estimates of clear-sky radiance for each channel, a temperature and humidity profile, and surface elevation. The data analyzed here are the Version-4 VIRS radiances for January 1998.

## 3. RETRIEVAL TECHNIQUE

A set of algorithms was developed to derive cloud height, optical depth, phase, effective particle size, and water path from these channels for each pixel. The main algorithm used during the daytime is the VIST (Visible Infrared Solar-Infrared Technique) described by Minnis et al. (1995). Given the clear-sky radiances for a particular set of solar zenith $\theta_o$, viewing zenith,

*_Corresponding author address_: Patrick Minnis, NASA Langley Research Center, MS 420, Hampton, VA 23681-2199. email: p.minnis@larc.nasa.gov.

and relative azimuth angles, the VIST computes the spectral radiances expected for both liquid-droplet and ice-water clouds for a range of optical depths $\tau$ = 0.25 to 128 for a particular cloud temperature $T_c$. The effective radii $r_e$ for the model clouds range from 2 to 32 μm and the effective diameters $D_e$ for the hexagonal ice column model clouds vary from 6 to 135 μm. The model cloud radiances are computed using the reflectance and emittance parameterizations of Minnis et al. (1998). The VIST matches the observed visible (0.65 μm), solar infrared (3.75 μm), and infrared (10.8 μm) radiances to the same quantities computed with the parameterizations and corrected to the top of the atmosphere. The process is iterative and computes results for both

| | Ocean | Land | Desert | Total |
|---|---|---|---|---|
| $z_c$ (km) | 4.6 | 5.9 | 4.8 | 4.9 |
| $\tau$ | 7.3 | 12.4 | 8.7 | 8.4 |
| $r_e$ (μm) | 16.2 | 13.1 | 11.3 | 15.5 |
| $D_e$ (μm) | 57.0 | 60.3 | 56.8 | 57.7 |
| % ice | 39.9 | 42.1 | 29.1 | 39.7 |

Table 1. Mean January 1998 VIRS cloud properties.

ice and liquid cloud particles. Phase is determined by a combination of tests that incorporate the final cloud temperature, the initially derived cloud altitude, and a reflectance ratio of 1.6 μm to 0.65 μm. The phase selection is also required to be physically reasonable. Thus, no ice clouds are allowed for $T_c$ > 273K and no liquid clouds are permitted for $T_c$ < 233K. Initial validation results (Young et al., 1998; Mace et al., 1998) show that the VIST ice-cloud property retrievals are in good agreement with in situ and radar-derived values of $D_e$, $\tau$, and ice water path *IWP*.

The cloud liquid water path *LWP* and *IWP* are derived from the retrieved values of $\tau$ and particle size. Cloud-top height is the altitude or pressure from the nearest vertical temperature profile that corresponds to $T_c$. The cloud thickness is defined using a set of crude empirical parameterizations based on $\tau$, $T_c$, and altitude. Cloud base height is defined as the difference between the cloud-top height and the thickness. The VIST is applied to all pixels having $\theta_o \leq 78°$. After analysis, the VIRS pixel results are convolved to match the corresponding CERES scanner pixel using the scanner's point spread function to weight the results. The properties are convolved according to altitude with only two layers permitted for a given CERES pixel. Four altitude layers are defined: low, 1100 to 700 hPa; low-middle, 700 – 500 hPa; high-middle, 500 – 300 hPa; and high, 300 – 50 hPa. This convolution procedure can include some higher clouds in lower layers and vice versa depending on the two cloud layers selected for the CERES pixel. The results reported here are based on averages using the convolved data.

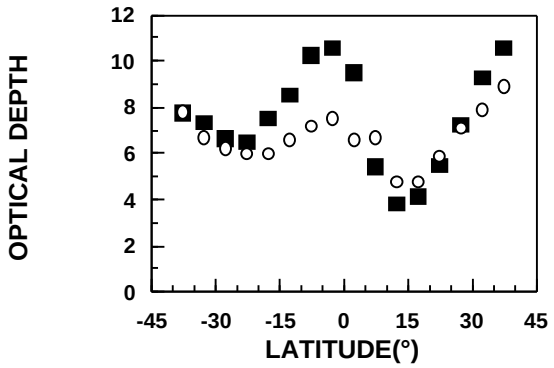


Fig. 1. Zonal mean January cloud optical depths from ISCCP (circles, 1986-93) and VIRS (squares, 1998).

## 4. RESULTS AND DISCUSSION

The mean daytime cloud parameter values from VIRS are summarized in Table 1. Of the 50.9% of the pixels classified as cloudy, 40% were categorized as ice clouds. The remaining 60% were determined to be primarily liquid water clouds and 13% of those were supercooled. The optical depths and cloud heights are significantly greater over land than elsewhere. Low clouds are more prevalent over the oceans and tropical deep convection is most vigorous over land areas like

the Amazon Basin. Figure 1 shows the variation of mean optical depth with latitude. The maxima occur around 5°S and 35°N. Maximum mean cloud heights of 7 km are found at 5°S, while the minimum cloud height of 3.3 km occurred in the northern subtropics near 20°N close to the minimum in $\tau$. The International Satellite Cloud Climatology Project (ISCCP) D2 mean optical depths for January 1986-93 show a similar zonal distribution except that the VIRS maximum is much greater. Overall, the ISCCP mean $\tau$ is 6.7, 20% smaller than the VIRS average. This difference may be due to natural variability, as January 1998 was part of an extreme El Nino period, to temporal sampling differences or to cloud amount differences. For example, the VIRS mean cloud amount is 18% less than the mean ISCCP values (Trepte et al. 1999). However, the VIRS and ISCCP cloud amounts are in closest agreement in the tropics and in the poorest agreement where the mean optical depths are the same.

Cloud effective droplet radius also depends on the surface type. The trend of decreasing $r_e$ (Table 1) with decreasing surface moisture is consistent with previous results from both in situ and satellite (e.g., Han et al. 1994) data. However, the mean values of $r_e$ exceed previous

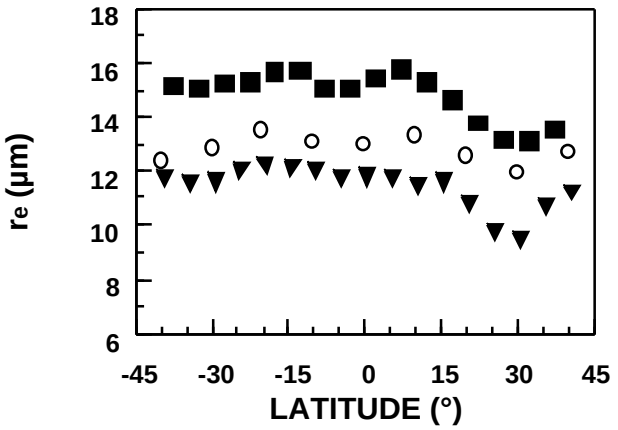


Fig. 2. Mean droplet effective radius from January 1987 AVHRR (Han et al. 1994, **P**; Minnis et al. 1997, **E**) and 1998 VIRS (**B**) data.

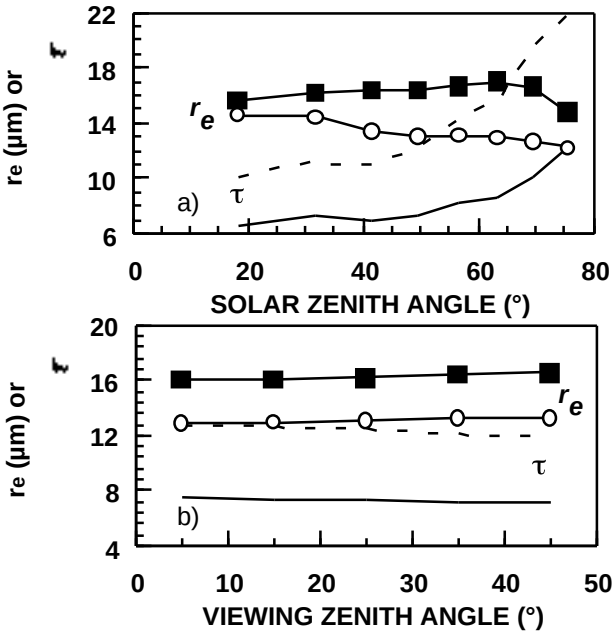


Fig. 3. Angular dependence of mean January 1998 effective radii and optical depth from VIRS over ocean (**B**, solid) and land (**E**, dashed).

results by 18 to 25%. The zonal means of $r_e$ from VIRS and from January 1987 NOAA-9 Advanced Very High Resolution Radiometer (AVHRR) data as analyzed by Han et al. (1994) and Minnis et al. (1997) in Fig. 2 show similar variations but distinct offsets. The Han et al. (1987) data are based only on near-nadir pixels with $T_c > 273$ K, while the Minnis et al. (1997) analysis used all angles, cloud temperatures identified as liquid, and no atmospheric corrections. The current analysis corrects for the atmospheric attenuation, all liquid cloud temperatures, and all angles. The NOAA-9 data were taken near 1500 local time (LT), while VIRS covers all times of day. There is essentially no dependence of $r_e$ on $\theta$ (Fig. 3b), and $r_e$ decreases with $\theta_o$ only over land (Fig. 3a). The atmospheric correction tends to decrease $r_e$ and the values of $r_e$ are larger for $T_c > 273$K than for colder temperatures. Initial validation of the VIRS results using surface-based radar data (Dong et al. (1999) show excellent agreement in $r_e$ for most single-layer cloud cases. Some

overestimate by VIRS is observed but it appears to occur whenever thin cirrus clouds are present.

Mean cloud optical depths show a much stronger dependence on $\theta_o$ than $r_e$. Over land and ocean, $\tau$ increases with increasing $\theta_o$ (Fig. 3a) doubling between 40° and 78°. Only a slight decrease in $\tau$ occurs with increasing $\theta$. The larger optical depths at high sun angle are probably due to a combination of effects. Some increase is expected due to the three-dimensional characteristics of real clouds. However, deep convection over most land areas peaks during the late afternoon and, over tropical oceans, during the early morning and late afternoon. The land cycle is consistent with a maximum in cloud height for $\theta_o$ > 65°. Furthermore, the diurnal cycle in marine stratocumulus clouds is marked by thicker clouds in early morning and evening with thinning during midday.

The effective ice crystal sizes are relatively independent of surface type (Table 1) but vary somewhat with latitude (Fig. 4). The mean value

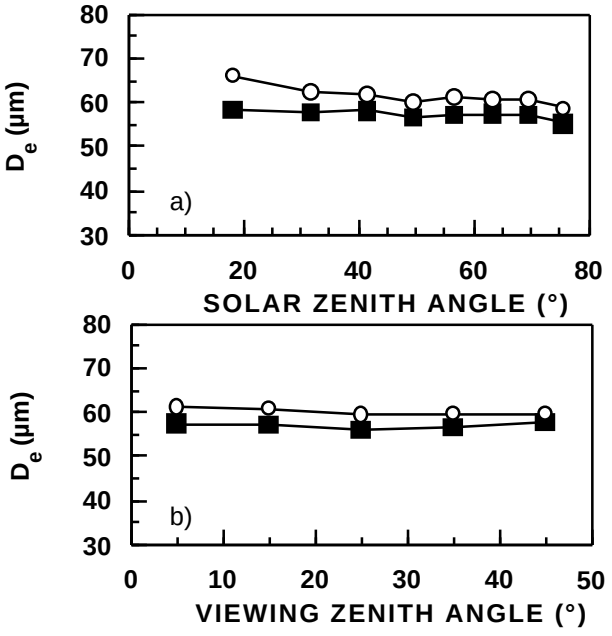


Fig, 4. Mean effective ice crystal sizes from January 1987 NOAA-9 (**E**, Minnis et al., 1997) and preliminary 1998 VIRS (**B**) data analyses.

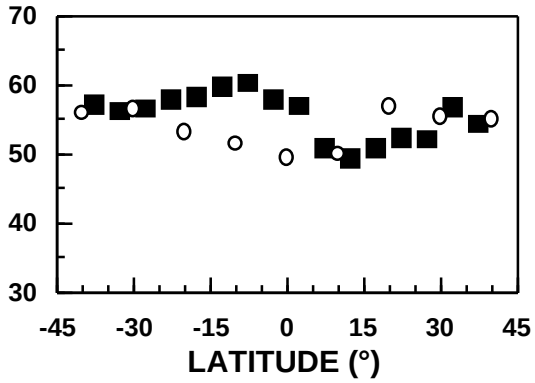


Fig. 5. Same as Fig. 3, except for effective ice crystal diameter; ocean (**B**), land (**E**).

of $D_e$ is minimally larger that from Minnis et al. (1997). However, the zonal variations are slightly different with the VIRS maximum between 5 and 10°S, the location of the minimum from 1987. This discrepancy may reflect the diurnal cycle as the largest crystals over land are seen at $\theta_o$ < 25° (Fig. 5a). No dependence of $D_e$ on $\theta$ is evident in Fig. 5b.

## 5. CONCLUDING REMARKS

The initial results from the CERES analysis of VIRS are, in general, consistent with previous retrievals of cloud properties from satellite measurements and the current understanding of the diurnal cycles of clouds. Much closer examination of the results is needed to understand the conditions when the retrievals disagree with other measurements. Additional algorithms are under development to improve the phase and particle size retrievals using the 1.6-μm channel and to include contextual information to detect pixels containing overlapped cloud fields and retrieve the properties more accurately in such conditions. An improved technique for detecting and analyzing the properties of thin clouds at night is also under development and will be implemented to achieve consistency in the retrieved cloud fields over the entire diurnal cycle. The VIRS cloud properties, however, can already

aid the goal of improved interpretation of CERES radiances and determination of the interaction between clouds and the radiation budget.

**References**


Dong, X., P. Minnis, S. Sun-Mack, G.G. Mace, E. E. Clothiaux, and C.N. Long, 1999: Validation of CERES/VIRS cloud property retrievals using ground-based measurements obtained at the DOE ARM sites. AMS 10th Conf. Atmos. Rad., Madison, WI, June 28 – July 2.

Han, Q., W. B. Rossow, and A. A. Lacis, 1994: Near-global survey of effective drop radii in liquid water clouds using ISCCP data. *J. Climate*, **7**, 465-497.

Mace, G. G., T. P. Ackerman, P. Minnis, and D. F. Young, 1998: Cirrus layer microphysical properties derived from surface-based millimeter radar and infrared interferometer data. *J. Geophys. Res.*, **103**, 23,207-23,216.

Minnis, P., D. P. Garber, D. F. Young, R. F. Arduini, and Y. Takano, 1998: Parameterization of reflectance and effective emittance for satellite remote sensing of cloud properties. *J. Atmos. Sci.*, **55**, 3313-3339.

Minnis, P., D. P. Kratz, J. A. Coakley, Jr., M. D. King, D. Garber, P. Heck, S. Mayor, D. F. Young, and R. Arduini, 1995: Cloud Optical Property Retrieval (Subsystem 4.3). "Clouds and the Earth's Radiant Energy System (CERES) algorithm theoretical basis document, Volume III: Cloud Analyses and Radiance Inversions (Subsystem 4)", *NASA RP 1376 Vol. 3*, pp. 135-176.

Minnis, P., D. F. Young, B. A. Baum, P. W. Heck, and S. Mayor, 1997: A near-global Analysis of cloud microphysical properties using multispectral AVHRR data. *Proc. AMS 9th Conf. Atmos. Radiation*, Long Beach, CA, Feb. 2-7, 443-446.

Trepte, Q., Y. Chen, S. Sun-Mack, P. Minnis, D. F. Young, B. A. Baum, P. W. Heck, 1999: Scene identification for the CERES cloud analysis subsystem. *Proc. AMS10th Conf. Atmos. Rad.*, 28 June – 2 July, Madison, WI.

Wielicki, B. A., B. R. Barkstrom, B. A. Baum, T. P. Charlock, R. N. Green, D. P. Kratz, et al., 1998: Clouds and the Earth's Radiant Energy System (CERES): Algorithm overview. *IEEE Trans. Geosci. Remote Sens.*, **36**, 1127-1141.

Young, D. F., P. Minnis, D. Baumgardner, and H. Gerber, 1998: Comparison of in situ and satellite-derived cloud properties during SUCCESS. *Geophys. Res. Lett.*, **25**, 1125-1128.